Table 3 Buckling load for a truncated hemisphere subjected to a unit displacement on the top edge (See Fig. 2)

Circumferential wave number j	Present work[a] 10 Elements	Present work[a] 20 Elements	Yao	Wu and Cheng	Radhamohan and Prasad	Navaratna et al.
	Shell geometry: $R/t = 480.0$; $\alpha = 23° 30'$					
	Dimensionless buckling load $P/Et * 10^4$					
38	—	13.074			12.97	7.00
39	13.043	13.024			12.93	6.88
40	13.028	13.009	13.4903	13.0567	13.16	6.93
41	13.046	13.028	—	—	—	—

[a] Very fine mesh is used near the ends.

Table 4 Buckling load for a truncated sphere subject to a unit load on the top edge

Circumferential at wave number j	Number of elements 10[a]	Number of elements 20[a]
	Shell geometry: $R/t = 480.0$; $\alpha = 23° 30'$	
	Dimensionless buckling load $P/Et * 10^4$	
38	11.888	12.050
39	11.833	11.995
40	11.808	11.972
41	11.813	11.980

[a] Very fine mesh is used near the ends.

and Cheng, and Radhamohan and Prasad. However, the results of Navaratna et al. are in considerable disagreement with all other works.

The last example considered is that of truncated hemisphere of Fig. 2 subjected to axial tensile load. The boundary conditions for the prebuckling analysis are the following: 1) $u = w = \beta = 0$, at the bottom edge of the shell, and 2) $\beta = 0$, at the top edge of the shell. The boundary conditions used for the buckling analysis are $u = v = w = \beta = 0$, at the top and bottom edges of the shell. The problem is solved with 10 and 20 elements using graded meshes and the nondimensional buckling load obtained is presented in Table 4.

Conclusions

The numerical results obtained demonstrate that the present refined finite element yields accurate buckling loads for various shell geometries and agrees very well with the results of other numerical methods except that of Ref. 1.

References

[1] Navaratna, D. R., Pian, T. H. H., and Witmer, E. A., "Stability Analysis of Shells of Revolution by the Finite Element Method," *AIAA Journal*, Vol. 6, No. 2, Feb. 1968, pp. 355–361.

[2] Radhamohan, S. K., "Nonlinear Stability of Thin Shells of Revolution," Ph.D. thesis, 1971, Dept. of Civil Engineering, Indian Institute of Technology, Kanpur, India.

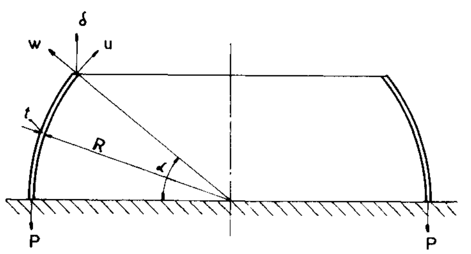

Fig. 2 Truncated hemispherical shell with axial tension.

[3] Bushnell, D., "Symmetric and Nonsymmetric Buckling of Finitely Deformed Eccentrically Stiffened Shells of Revolution," *AIAA Journal*, Vol. 5, No. 8, Aug. 1967, pp. 1455–1462.

[4] Yao, J. C., "Buckling of a Truncated Hemisphere under Axial Tension," *AIAA Journal*, Vol. 1, No. 10, Oct. 1963, pp. 2316–2319.

[5] Wu, M. T. and Cheng, S., "Nonlinear Asymmetric Buckling of Truncated Spherical Shells," *Transactions of the ASME, Journal of Applied Mechanics*, Vol. 37, series E, No. 3, Sept. 1970, pp. 651–660.

[6] Radhamohan, S. K. and Prasad, B., "Asymmetric Buckling of Toroidal Shells under Axial Tension," *AIAA Journal*, to be published.

[7] Sanders, J. L., "Nonlinear Theories for Thin Shells," *Quarterly of Applied Mathematics*, Vol. 21, No. 1, 1963, pp. 21–36.

[8] Adelman, H. M., Catherines, D. S., and Walton, W. C., Jr., "A Method for Computation of Vibration Modes and Frequencies of Orthotropic Thin Shells of Revolution Having General Meridional Curvature," TN D.4972, Jan. 1969, NASA.

[9] Hoff, N. J. and Soong, T. C., "Buckling of Circular Cylindrical Shells in Axial Compression," *International Journal of Mechanical Sciences*, Vol. 7, July 1965, pp. 489–520.

[10] Simmonds, J. G. and Danielson, D. A., "New Results for the Buckling Loads of Axially Compressed Cylindrical Shells Subjected to Relaxed Boundary Conditions," *Transactions of the ASME, Journal of Applied Mechanics*, Vol. 37, Series E, No. 1, March 1970, pp. 93–100.

Solution for Inplane and Bending Fields of Tapered Anisotropic Conical Shells

JOSEPH PADOVAN*
University of Akron, Akron, Ohio

Introduction

RECENTLY Padovan has developed exact solutions for anisotropic laminated cylindrical shells,[1–3] plate strips,[4] circular plates[5,6] and half-space problems.[7,8] Outside of these configurations little is known about the effects of curvilinear material anisotropy. With this in mind, the present Note develops an exact solution for the static mechanical loading of anisotropic tapered conical shells with arbitrary edge conditions. In particular the type of taper treated is linearly dependent on the usual meridional variable used for conical shells.[9]

To illustrate the solution procedure, Donnell type cone equations[9] are used. For the isotropic case, the solution developed herein, reduces to the Donnell form of those given by Flugge.[9] Based on the generality of the solution procedure, the following effects can also be incorporated in the present

Received May 11, 1973; revision received August 13, 1973.
Index category: Structural Static Analysis.

* Assistant Professor of Mechanical Engineering.

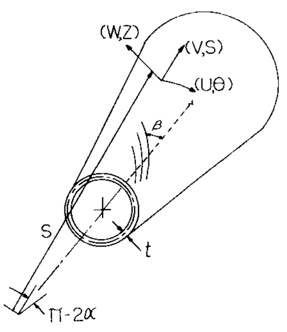

Fig. 1 Tapered conical shell geometry.

treatment: 1) arbitrary laminate configuration; 2) individually anisotropic lamina; 3) shear deformation; 4) Flugge type shell theory.[9]

Geometry

In terms of Fig. 1, the position of a point of a cone is defined by s the distance measured from the apex, θ the circumferential coordinate and z measured perpendicular to the reference surface such that $z\varepsilon[-t/2,\ t/2]$. The components of displacement of such a point are defined by u, v and w in the θ, s and z directions, respectively. In terms of the introduction, the type of wall thickness variation treated is defined by

$$t = \delta s \tag{1}$$

Constitutive Equations

For the cone configuration considered herein, the Donnell type constitutive equations are given by

$$\begin{bmatrix} N_s \\ N_\theta \\ N_{\theta s} \end{bmatrix} = s \begin{bmatrix} A_{11} & A_{12} & A_{16} \\ A_{12} & A_{22} & A_{26} \\ A_{16} & A_{26} & A_{66} \end{bmatrix} \mathbf{x} \tag{2}$$

$$\begin{bmatrix} M_s \\ M_\theta \\ M_{\theta s} \end{bmatrix} = s^3 \begin{bmatrix} D_{11} & D_{12} & D_{16} \\ D_{12} & D_{22} & D_{26} \\ D_{16} & D_{26} & D_{66} \end{bmatrix} \boldsymbol{\eta} \tag{3}$$

such that

$$\mathbf{x} = \begin{bmatrix} v,_s \\ 1/s[(1/\cos\alpha)u,_\theta + v + w\tan\alpha] \\ \{u,_s - (1/s)u + [1/(s\cos\alpha)]v,_\theta\} \end{bmatrix} \tag{4}$$

and

$$\boldsymbol{\eta} = \begin{bmatrix} w,_{ss} \\ [1/(s^2\cos^2\alpha)]w,_{\theta\theta} + (1/s)w,_s \\ [(1/s)w,_{s\theta} - (1/s^2)w,_\theta]/\cos\alpha \end{bmatrix} \tag{5}$$

where $(\ ),_s$ denotes partial differentiation; $N_s, \ldots$ are inplane resultants; $M_s, \ldots$ bending resultants and A_{lk}, D_{lk} are stiffness elements defined by

$$A_{lk} = \delta E_{lk} \tag{6}$$

$$D_{lk} = (\delta^3/12)E_{lk} \tag{7}$$

with E_{lk} being 3-D stiffnesses. As the cone is considered anisotropic, $[A_{lk}]$ and $[B_{lk}]$ are fully populated.

Equations

Consistent with Eqs. (2–5), the Donnell type equilibrium equations for the cone are given by[9]

$$s(sN_{s\theta}),_s + sN_{\theta,\theta}\sec\alpha + sN_{\theta s} - (sM_{\theta s}),_s \tan\alpha - M_{\theta s}\tan\alpha - M_{\theta,\theta}\tan\alpha\sec\alpha = -s^2 P_\theta \tag{8}$$

$$(sN_s),_s + N_{\theta s,\theta}\sec\alpha - N_\theta = -sP_s \tag{9}$$

$$sN_\theta\tan\alpha + s(sM_s),_{ss} + 2(sM_{\theta s,\theta}),_s\sec\alpha + M_{\theta,\theta\theta}\sec^2\alpha - sM_{\theta,s} = s^2 P_r \tag{10}$$

where P_r, P_θ and P_s are, respectively, surface tractions in the r, θ and s coordinate directions. Employing Eqs. (2–5), the equilibrium equations can be recast in displacement form. Through the use of matrix notation, the basic form of such equations can be revealed. Hence, Eqs. (2–10) can be recast as follows

$$s^4\mathbf{G}_1\xi,_{ssss} + s^3\mathbf{G}_2\xi,_{sss\theta} + s^2\mathbf{G}_3\xi,_{ss\theta\theta} + s\mathbf{G}_4\xi,_{s\theta\theta\theta} + \mathbf{G}_5\xi,_{\theta\theta\theta\theta} + s^3\mathbf{G}_6\xi,_{sss} + s^2\mathbf{G}_7\xi,_{ss\theta} + s\mathbf{G}_8\xi,_{s\theta\theta} + \mathbf{G}_9\xi,_{\theta\theta\theta} + s^2\mathbf{G}_{10}\xi,_{ss} + s\mathbf{G}_{11}\xi,_{s\theta} + \mathbf{G}_{12}\xi,_{\theta\theta} + s\mathbf{G}_{13}\xi,_s + \mathbf{G}_{14}\xi,_\theta + \mathbf{G}_{15}\xi + \mathbf{F} = 0 \tag{11}$$

The coefficients $\mathbf{G}_1, \ldots, \mathbf{G}_{15}$ appearing in Eq. (11) are three by three real matrices such that $\mathbf{G}_1, \ldots, \mathbf{G}_5$ are singular and ξ and $\mathbf{F}$ are given by

$$\xi = \{u, v, w\}^T \tag{12}$$

$$\mathbf{F} = \{P_\theta, P_s, P_r\}^T \tag{13}$$

The boundary conditions associated with Eq. (11) on $s =$ constant surfaces are given by

$$\begin{aligned} N_s \pm \kappa_1 v &= \tilde{N}_s \\ N \pm \kappa_2 u &= \tilde{N} \\ M_s \pm \kappa_3 w,_s &= \tilde{M}_s \\ Q \pm \kappa_4 w &= \tilde{Q} \end{aligned} \tag{14}$$

where the overwavy bar denotes prescribed quantities; N and Q are effective quantities and κ_i can be so chosen as to yield displacement, traction or spring type edge conditions.

Solution

From the manner of appearance of s, Eqs. (11) are seen to be Euler type *PDE*. Hence, by letting

$$s = e^x \tag{15}$$

Eqs. (11) can be reduced to

$$\mathbf{Q}_1\xi,_{xxxx} + \mathbf{Q}_2\xi,_{xxx\theta} + \mathbf{Q}_3\xi,_{xx\theta\theta} + \mathbf{Q}_4\xi,_{x\theta\theta\theta} + \mathbf{Q}_5\xi,_{\theta\theta\theta\theta} + \mathbf{Q}_6\xi,_{xxx} + \mathbf{Q}_7\xi,_{xx\theta} + \mathbf{Q}_8\xi,_{x\theta\theta} + \mathbf{Q}_9\xi,_{\theta\theta\theta} + \mathbf{Q}_{10}\xi,_{xx} + \mathbf{Q}_{11}\xi,_{x\theta} + \mathbf{Q}_{12}\xi,_{\theta\theta} + \mathbf{Q}_{13}\xi,_x + \mathbf{Q}_{14}\xi,_\theta + \mathbf{Q}_{15}\xi + \mathbf{F} = \mathbf{0} \tag{16}$$

where $\mathbf{Q}_1, \ldots, \mathbf{Q}_{15}$ are given by

$$\begin{aligned} &\mathbf{Q}_i = \mathbf{G}_i;\quad i = 1,2,\ldots,5 && \mathbf{Q}_{11} = \mathbf{G}_{11} + 2\mathbf{G}_2 - \mathbf{G}_7 \\ &\mathbf{Q}_6 = \mathbf{G}_6 - 6\mathbf{G}_1 && \mathbf{Q}_{12} = \mathbf{G}_{12} \\ &\mathbf{Q}_7 = \mathbf{G}_7 - 3\mathbf{G}_2 && \mathbf{Q}_{13} = \mathbf{G}_{13} - 6\mathbf{G}_1 + 2\mathbf{G}_6 - \mathbf{G}_{10} \\ &\mathbf{Q}_8 = \mathbf{G}_8 - \mathbf{G}_3 && \mathbf{Q}_{14} = \mathbf{G}_{14} \\ &\mathbf{Q}_9 = \mathbf{G}_9 && \mathbf{Q}_{15} = \mathbf{G}_{15} \\ &\mathbf{Q}_{10} = \mathbf{G}_{10} + 11\mathbf{G}_1 - 3\mathbf{G}_6 \end{aligned} \tag{17}$$

In its present general form, Eq. (16) is noncanonical. Furthermore, due to the appearance of the E_{16}, E_{26} stiffnesses, the standard Fourier decomposition cannot be used to yield a solution of Eqs. (14 and 16).[9] Following Padovan,[1–3] due to the periodicity of the θ coordinate, it follows that for $\mathbf{F}$ which satisfy Dirichlet's condition, ξ and $\mathbf{F}$ can be formally expanded in complex Fourier series. Hence

$$\langle \xi, \mathbf{F} \rangle = \sum_{m=-\infty}^{\infty} \langle \xi_m, \mathbf{F}_m \rangle e^{jm\theta} \tag{18}$$

where $j = (-1)^{1/2}$ and

$$\langle \xi_m, \mathbf{F}_m \rangle = \frac{1}{2\pi} \int_0^{2\pi} \langle \xi, \mathbf{F} \rangle e^{-jm\theta}\, d\theta \tag{19}$$

Transforming Eqs. (14) and (16) with Eq. (19) yields the following set of complex equations

$$\mathbf{Q}_1\xi_{m,xxxx} + [\mathbf{Q}_6 + jm\mathbf{Q}_2]\xi_{m,xxx} + [\mathbf{Q}_{10} - m^2\mathbf{Q}_3 + jm\mathbf{Q}_7]\xi_{m,xx} + [\mathbf{Q}_{13} - m^2\mathbf{Q}_8 + j(m\mathbf{Q}_{11} - m^3\mathbf{Q}_4)]\xi_{m,x} + [\mathbf{Q}_{15} + m^4\mathbf{Q}_5 - m^2\mathbf{Q}_{12} + j(m\mathbf{Q}_{14} - m^3\mathbf{Q}_9)]\xi_m + \mathbf{F}_m = \mathbf{0} \tag{20}$$

and

$$\begin{aligned} N_{sm} \pm \kappa_1 v_m &= \tilde{N}_{sm} \\ N_m \pm \kappa_2 u_m &= \tilde{N}_m \\ M_{sm} \pm \kappa_3 w_{m,s} &= \tilde{M}_{sm} \\ Q_m \pm \kappa_4 w_m &= \tilde{Q}_m \end{aligned} \tag{21}$$

Contrary to the isotropic[9] or orthotropic cases, for nonzero E_{16} and E_{26}, Re $\{\xi_m\}$ and Im $\{\xi_m\}$ are coupled.

Irrespective of their complex form, the homogeneous solution of Eqs. (20 and 21) takes the form

$$\xi_m = \sum_{i=1}^{8} \alpha_{mi} \zeta_{mi} e^{\lambda_{mi} x} \tag{22}$$

where λ_{mi} and ζ_{mi} are latent roots and vectors of the following irregular complex fourth order polynomial matrix

$$\{\lambda_{mi}^4 \mathbf{Q}_1 + \lambda_{mi}^3 [\mathbf{Q}_6 + jm\mathbf{Q}_2] + \lambda_{mi}^2 [\mathbf{Q}_{10} - m^2 \mathbf{Q}_3 + jm\mathbf{Q}_7] + \lambda_{mi} [\mathbf{Q}_{13} - m^2 \mathbf{Q}_8 + j(m\mathbf{Q}_{11} - m^3 \mathbf{Q}_4)] + [\mathbf{Q}_{15} + m^4 \mathbf{Q}_5 - m^2 \mathbf{Q}_{12} + j(m\mathbf{Q}_{14} - m^3 \mathbf{Q}_9)]\} \zeta_{mi} = \mathbf{0} \tag{23}$$

By taking the determinant of the pencil of Eq. (23), the following complex characteristic polynomial is obtained

$$\sum_{i=0}^{8} g_i \lambda^{8-i} = 0 \tag{24}$$

such that g_i are complex constants. For the isotropic[9] and orthotropic cases, $g_1, g_3, \ldots, g_7$ reduce to zero. The constants α_{mi} appearing in Eq. (22) are obtained by satisfying the transformed boundary conditions denoted by Eq. (21).

Since Eq. (23) has a complex pencil, its latent roots and associated latent vectors no longer occur in conjugate pairs for a given m value. However, due to its inherent functional dependency, it follows from Eq. (23) that

$$\bar{\lambda}_{mi} = \lambda_{-mi} \tag{25}$$

and

$$\bar{\zeta}_{mi} = \zeta_{-mi} \tag{26}$$

Furthermore, based on the transformed boundary conditions and Eqs. (25 and 26), it also follows that

$$\bar{\alpha}_{mi} = \alpha_{-mi} \tag{27}$$

Hence, in terms of Eqs. (18, 22 and 25–27), ξ is given by

$$\xi = \sum_{i=1}^{8} \alpha_{0i} \zeta_{0i} s^{\lambda_{0i}} + \sum_{m=1}^{\infty} \sum_{i=1}^{8} 2 [\mathrm{Re}(\alpha_{mi} \zeta_{mi}) \cos(\mathrm{Im}(\lambda_{mi}) \ln s + m\theta) - \mathrm{Im}(\alpha_{mi} \zeta_{mi}) \sin(\mathrm{Im}(\lambda_{mi}) \ln s + m\theta)] s^{\mathrm{Re}(\lambda_{mi})} \tag{28}$$

The inplane and bending resultant fields can be directly obtained by substituting Eq. (28) into Eqs. (2) and (3), respectively. Since the procedure used to develop the solution is basically an extension of the Levy technique used for classical isotropic and orthotropic problems, the convergence of Eq. (28) is directly dependent on the number of terms needed to represent the various boundary conditions and surface tractions in standard Fourier series.

Example

As an example of the possible effects of material anisotropy the following boundary value problem is considered

$$\begin{aligned} s = 15'' \text{ or } 36'' \qquad & u = v = w \equiv 0 \\ P_r = \sigma \cos\theta \qquad & P_\theta = P_s = 0 \end{aligned} \tag{29}$$

where $\alpha = 60°$, $\delta = 1/150$, and β the local material orientation depicted in Fig. 1 is chosen as either 0° or 45°. For the present study the latent roots and vectors of Eq. (23) were obtained by recasting Eq. (24) as a complex eigenvalue problem which can be solved using standard eigenvalue procedures.[1-3] The computational times needed to evaluate the said eigenvalue problems were essentially the same as those required to obtain the roots of classical isotropic and orthotropic problems.[9] Figure 2 presents the significant effects of α on the N_s field. Similar redistributions are also noted for the remaining field variables.

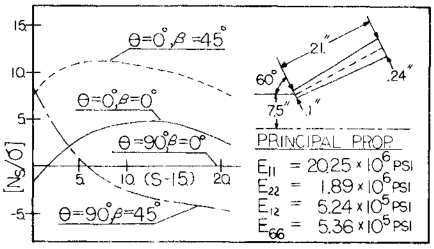

Fig. 2 Effects of β on N_s field of tapered cone.

References

[1] Padovan, J., "Frequency and Buckling Eigenvalues of Anisotropic Cylinders Subjected to Nonuniform Lateral Prestress," *International Journal of Solids and Structures*, Vol. 7, 1971, pp. 1449–1466.

[2] Padovan, J. and Lestingi, J., "Mechanical Behavior of Fiber Reinforced Cylinders," *AIAA Journal*, Vol. 10, No. 9, Sept. 1972, pp. 1239–1241.

[3] Padovan, J., "Natural Frequencies of Rotating Prestressed Cylinders," *Journal of Sound and Vibration*, (in press, Dec. 1973).

[4] Padovan, J., "In Plane and Bending Fields of Anisotropic Generally Laminated Plate Strips," *Journal of Composite Materials* (in press).

[5] Padovan, J. and Lestingi, J., "Static Solution of Monoclinic Circular Plates," *AIAA Journal*, Vol. 9, No. 12, Dec. 1971, pp. 2473–2474.

[6] Padovan, J. and Lestingi, J., "Natural Frequencies of Monoclinic Circular Plates," *Journal of the Acoustical Society of America*, to be published.

[7] Padovan, J., "Stresses in an Anisotropic Half Space," *AIAA Journal*, Vol. 11, No. 8, Aug. 1973, pp. 1194–1195.

[8] Padovan, J., "Thermoelasticity of an Elastic Anisotropic Half Space," *Proceedings of the Fourth Canadian Congress of Applied Mechanics*, Montreal, May 28–June 1, 1973, pp. 73–74.

[9] Flugge, W., *Stresses in Shells*, Springer-Verlag, New York, 1967, pp. 396–407.

Simple Spectroscopic Technique for the Arc Region of Plasma Accelerators

ROBERT P. COLLIER* AND DAVID S. SCOTT†
University of Toronto, Toronto, Ontario, Canada

Introduction

THE application of spectroscopic diagnostic techniques to plasma accelerator exhaust plumes is well known and documented.[1-6] However, the use of spectroscopy in the accelerator arc region has been quite limited. This results, primarily, from the lack of convenient optical access to the discharge region. One solution to this problem has been that of Grossman[7] who used an anode in which viewing ports had been drilled to obtain spectroscopic data yielding average temperature and density in the arc region. Bohn, Beth, and Nedder[2] have suggested a modified Abel inversion technique which allows transformation of data obtained at angles not perpendicular to the plasma axis.

Received June 13, 1973; revision received August 16, 1973.

Index categories: Plasma Dynamics and MHD; Electric and Advanced Space Propulsion; Radiation and Radiative Heat Transfer.

* Research Associate, Department of Mechanical Engineering. Student Member AIAA.

† Associate Chairman, Department of Mechanical Engineering.